Carbon Science

Vol. 4, No. 1 March 2003 pp. 10-13

Studies on Nanostructured Amorphous Carbon by X-ray Diffraction and Small Angle X-ray Scattering

K. Dasgupta♠, P. S. R. Krishna*, R. Chitra* and D. Sathiyamoorthy

Materials Processing Division, Bhabha Atomic Research Centre, Mumbai 400 085, India
*Solid State Physics Division, Bhabha Atomic Research Centre, Mumbai 400 085, India
♠e-mail: *kdg@magnum.barc.ernet.in*

(Received May 10, 2002; accepted July 17, 2002)

Abstract

The structural studies of amorphous isotropic carbon prepared from pyrolysis of phenol formaldehyde resin have been carried out using X-ray diffraction. X-ray diffraction from as prepared sample at 1000°C and a sample treated at 1900°C revealed that both are amorphous even though there are small differences in short range order. It is found that both are graphite like carbon (GLC) with predominantly sp^2 hybridization. Small angle X-ray scattering results show that as prepared sample mainly consists of thin two dimensional platelets of graphitic carbon whereas they grow in thickness to become three dimensional materials of nano dimensions.

Keywords : *isotropic carbon, pyrolysis, small angle X-ray scattering, X-ray diffraction*

1. Introduction

Carbon derived from the pyrolysis of organic substances may be ordered or disordered in nature depending on structure of the precursor material [1]. The disordered or amorphous carbon can have wide range of properties depending on the ratio of sp^2 and sp^3 hybridization. Amorphous carbon with substantial amount of sp^2 hybridization is known as graphite-like carbon (GLC) and those with more of sp^3 hybridization are known as diamond-like carbon (DLC). Amorphous carbons produced by controlled pyrolysis of organic precursors generally consist of carbon in a GLC form [2]. The resulting structures have normally a high surface area due to the micro- and meso-porosity. It is this feature that makes amorphous carbon useful for a wide range of commercial applications.

Graphite is used in nuclear reactors operating at high temperature, where the radiation defects are annealed out and strain energy is not accumulated. In thermal nuclear reactors due to the accumulation of Wigner energy [3] graphite cannot be used. Wigner energy is the strain energy which is stored in graphite due to the displacement of atoms from lattice positions as a result of irradiation. Amorphous isotropic carbon can be used as a scatterer material for neutrons in thermal reactors where this accumulation of Wigner energy should not arise. There are certain carbon materials that are amorphous at lower temperature range (< 900°C) but graphitize (crystallize) when heated to higher temperature. In the present studies, our objective is to prepare an amorphous carbon which should not graphitize (crystallize) even at high temperature. Hence an attempt was made to prepare amorphous carbon by carbonizing the precursor phenol formaldehyde at 1000°C (Sample A) and further heat treatment at 1900°C (Sample B).

In this paper we present the results of X-ray diffraction (XRD) to understand the short range order and that of small angle X-ray scattering (SAXS) to understand the mesoscopic structure in this carbon.

2. Theoritical Background

2.1. X-Ray Diffraction from amorphous materials

The radial distribution function (RDF) $4\pi r^2\rho(r)$, is used to characterize amorphous structures. It represents the number of atoms in a spherical shell of radius r having unit thickness. The function RDF is zero for values of r less than the hard sphere diameter of the atoms and modulates about $4\pi r^2\rho_0$ for larger values of r, where ρ_0 is the average atomic density in the amorphous material under consideration. Peaks in the plot of RDF vs r correspond to the frequently occurring atom-atom distances and the area under the peak is equal to the average number of atom pairs within the particular range of distances [4]. The interference function [5] I(Q) is given by

$$I(Q) = \left[I_a^{coh}(Q) - \sum_i^n x_i f_i^2(Q) \right] \left[\sum_i^n x_i f_i(Q) \right]^{-2} \qquad (1)$$

where $Q=4\pi\ (\sin\theta)/\lambda$, 2θ is the scattering angle, λ is the

wavelength, f_i the atomic scattering factor, x_i the molar fractions of the component, n the number of atomic species and $I_a^{coh}(Q)$ is the coherently scattered intensity in electron units.

Reduced RDF is defined as $G(r)=4\pi r[\rho(r)-\rho_0]$. Fourier transformation of the function $QI(Q)$ gives

$$G(r) = (2/\pi)\int_0^\infty QI(Q)\sin(Qr)dQ \quad (2)$$

2.2. Small Angle X-Ray Scattering (SAXS)

SAXS is a technique used for characterizing objects on a scale of lengths 10 Å to 10000 Å and also of objects which are fractals. The expression for the SAXS intensity of a dilute dispersion of particles may be approximated as [6]:

$$I(Q) = I_0\exp(-R_g^2 Q^2/3) \quad (3)$$

where R_g is the radius of gyration. Standard expressions of R_g are available for regularly shaped simple uniform particles in the literature [7]. A plot of ln $I(Q)$ *vs.* Q^2 yields R_g^2 (which is known as Guinier plot).

The intensity $I(Q)$ of the small angle scattering from a mass fractal with fractal dimension D can be written [8, 9] as

$$I(Q) = I_0\Gamma(D+1)\{\sin[\pi(D-1)/2]/(D-1)\}Q^{-D} \quad (4)$$

where I_0 is a constant that depends on both the experimental conditions and the structure of the fractal and $\Gamma(x)$ is the gamma function. The above equation is valid if $Q\xi >> 1$, where ξ is the diameter of the fractal [10].

3. Experimental

Samples were made from phenol formaldehyde resin (resol type) supplied by Marvel Thermosets Pvt. Ltd, India (PLGW-8 grade). The liquid resin was cured into solid form. This solid resin was cut into small pieces. These pieces were heated to 1000°C in argon atmosphere with a heating rate of 100°C/hr in the temperature range of 200°C to 700°C. The carbonized sample was milled into fine powders using pot mill and planetary mill. For diffraction purpose very fine particles having median diameter of 3 micron were taken. These particles were leached with acid to remove the contamination from milling. The leached sample (Sample A), treated at 1000°C was used for XRD. Some amount of the leached powder was further heat treated to 1900°C in argon atmosphere using induction furnace. This sample (Sample B) has also been studied.

X-ray diffraction of the carbon samples was carried out in the Bragg-Brentano geometry with a pyrolytic graphite monochromator in the scattered beam on the Rigaku rotating anode X-ray diffractometer. The samples were kept in such a way that there was no back plate to avoid substrate scattering contamination and the thickness of the samples was about 2.5 mm. The radiation used was Molybdenum K_α which has a shorter wave length (≈0.7107 Å) and thus facilitates higher Q-range which is required to understand the short range order. Data were collected in the scattering angle range from 2° to 145° increased in steps of 0.05° using proper divergence slits to make sure that the beam size stays within the sample. SAXS experiments were performed on these samples in transmission geometry in the angular range (2θ) of 0.07 to 3.5 using the small angle attachment.

In order to understand the mesoscopic structure of this sample, we used the SAXS data. The diffraction data have been analyzed using the well known RAD program [11] to get the structure factor and the radial distribution function, (RDF).

These samples were also characterized by optical microscopy. Polarized light with cross polarizers and lambda plate was used to ensure their amorphous and isotropic nature within optical resolution [12].

4. Results and Discussion

Figures 1 shows the optical microstructure of the carbon samples treated at 1900°C (sample B). The typical interference colour indicates that this sample is isotropic and disordered in the optical resolution scale [12].

The modified interference function, $QI(Q)$, of both the samples A and B have been shown in the Figure 2. It can be seen that both the samples are X-ray amorphous with no Bragg peaks (*i.e.* sharp). Sample B shows relatively sharper peaks in the $QI(Q)$ which shows that the coherently scattering domain size is bigger for Sample B. The calculated RDF is shown in the Figure 3.

The peaks in RDF are sharper in the case of sample A showing that the distribution of the bond distances is sharp in this sample. The first and second peaks in RDF have been

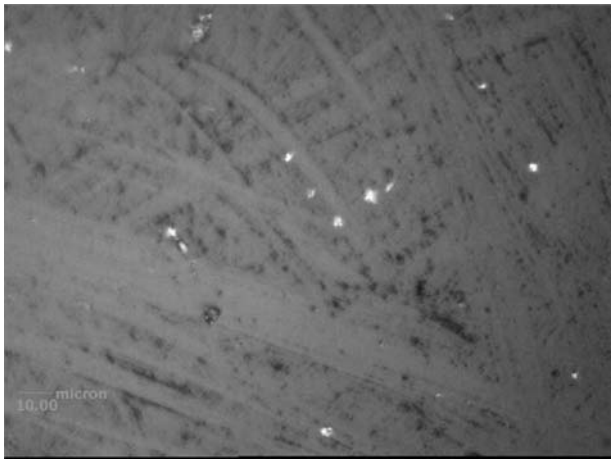

Fig. 1. Optical micrograph of the sample B showing typical interference colour of an isotropic sample.

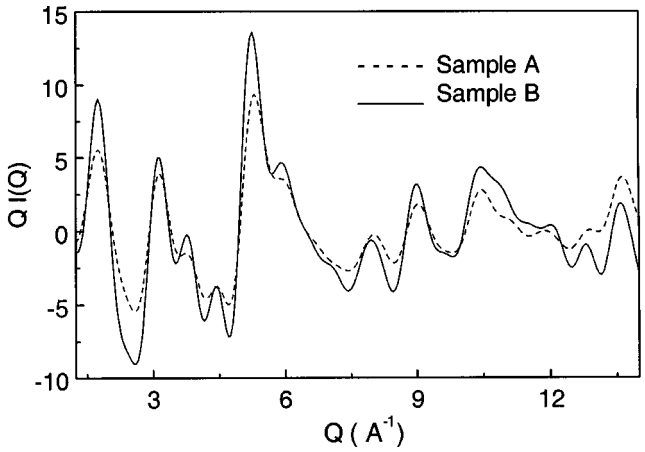

Fig. 2. The modified interference functions for the samples A (1000°C) and B (1900°C).

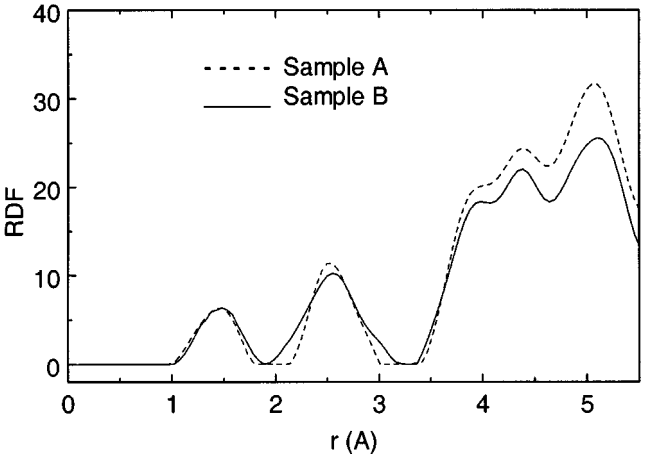

Fig. 3. The radial distribution functions for the samples A and B.

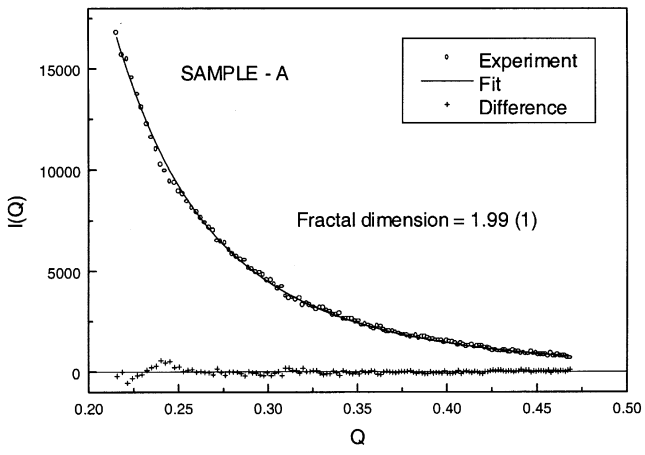

Fig. 4. SAXS data from sample A. Line is the fit to data (○) using equation 4 (see text). Also shown is the difference plot (+) between the data and fit.

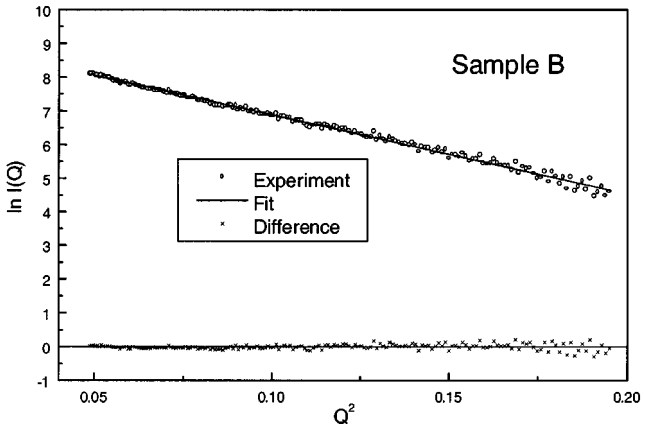

Fig. 5. SAXS data from sample B. Line is the fit to data (○) using cylindrical particles as a model using equation 3 (see text). Also shown is the difference plot (+) between the data and fit. The values for the cylinder radius and height are 7.8 Å and 21.8 Å respectively.

analyzed and the results for both the samples A and B are shown in the Table 1 along with few other reported values for various types of amorphous carbons. These data suggest that our carbon samples A and B are predominantly graphite like carbons even though they are slightly different from each other.

The SAXS data analysis shows the important structural differences in the meso-scale in both the carbons. We show the fitting of the equation (4) to the SAXS data in Figure 4 for sample A to get the fractal dimension which incidentally is about 1.99 (1). These results indicate that scattering mesoscopic objects are plate like with very small thickness in the case of sample A. This result coupled with the short range order of sample A leads to the conclusion that it mainly consists of graphite like sheets of very small thickness.

On the other hand the ln *I vs.* Q^2 plot (Guinier plot [6]) of sample B shows a large linear range as seen in Figure 5.

Table 1. Parameters for first and second peaks. r_1 and r_2 are the positions, and N_1 and N_2 are the co-ordination numbers of the first and second peaks respectively. θ is the bond angle. The number in the bracket ( ) indicates error in the last significant digit

Parameters	Graphite [13]	a-C (sputter) [14]	a-C [2]	Sample A	Sample B
r_1 (Å)	1.42	1.46	1.45(1)	1.40(1)	1.46(1)
r_2 (Å)	2.46	2.49	2.49(1)	2.52(1)	2.55(1)
θ (degree)	120.0	117.0	118.3	119.3	121.7
N_1	3.00	3.34	3.10(1)	2.90(1)	3.10(1)
N_2	6.00	6.81	6.30(2)	5.90(2)	6.30(2)

Analysis of this data suggests that the shape of these particles is like cylinders with a radius of 7.8 Å and a height of 21.8 Å. These results also explain why the peaks in the modified interference function, $QI(Q)$, are sharper for this sample as compared with sample A. This result coupled with the short range order of sample B leads to the conclusion that this sample is like nanocrystalline graphite but has sufficient disorder due to high surface to volume ratio (~35%).

5. Conclusions

Studies were carried out using optical microscopy, X-ray diffraction and small angle X-ray scattering measurements for the amorphous carbon obtained by carbonizing phenol formaldehyde at 1000^{o}C (sample A) and the heat treated sample at 1900^{o}C (sample B). Analysis showed that two samples are graphite like amorphous carbons. In the optical length scales both samples are amorphous in nature. As regards to mesoscopic length scales, sample A is found to be made up of thin graphite like sheets where as sample B is made up of cylindrical shaped graphitic particles of nano crystalline dimensions. The microscopic length scales probed by X-ray diffraction gives us the result that both are graphite like carbons and they have predominantly sp^2 hybridization.

Acknowledgement

The authors are grateful to Dr. S. Banerjee, Director, Materials Group and Dr. A. K. Suri, Head, Materials Processing Division, Bhabha Atomic Research Centre for supporting the ongoing program. They would like to thank Mrs. Ramani Venugopalan and Mr. S. M. Shetty of Materials Processing Division, Bhabha Atomic Research Centre for their technical help at various stages of investigation of the carbon samples.

References

[1] Franklin, R. E. *Proc. R. Soc.Lond* A **1957**, *209*, 196-218.
[2] Krishna, P. S. R.; Balaya, P.; Dasannacharya, B. A.; Ahmed Sayeed, Meenakshi, V.; Subramanyam, S. V. *Physica B* **1998**, *241-243***,** 921-923.
[3] Graphite Moderator Lifecycle Behavior, *IAEA Tecdoc-901* **1998**, 32-36.
[4] Klug, H. P.; Alexander, L. E. *X-ray Diffraction Procedures*, New York: Wiley, 1954.
[5] Pings, C. J.; Washer, J. J. *Chem. Phys*. **1968**, *48*, 3016-3018
[6] Guinier, A.; Fournet, G. *Small Angle Scattering of X-rays*. New York: Wiley, 1955.
[7] Feigin, L. A.; Svergun, D. I. In Taylor, G. W. editor. Structural Analysis by Small Angle X-ray and Neutron Scattering, New York: Plenum, 1987.
[8] Sinha, S. K.; Freeltojt, T.; Kjens, J. K., In Family, Landau DP editor. Kinetics of Aggregation and.
[9] Teixeira, J. *J. Appl. Cryst*. **1988**, *21*, 781-785.
[10] Schmidt, P. W. *J. Appl. Cryst.* **1991**, *24*, 414-435.
[11] Petkov, V. *J. Appl. Cryst.* **1989**, *2*, 387-389.
[12] Oberlin, A.; Bonnamy, S.; Lafdi, K. Structure and Texture of Carbon Fibers. In Donnet, J. B., Wang, T. K., Rebonillat, S., Peng, J. C. M. Editor. Carbon Fibers, 3rd edition, New York: Dekker, **1998**, 85-159.
[13] Robertson, J. *Adv. Phys.* **1986**, *35*, 317-374.
[14] Li, F.; Lannin, J. S. *Phys. Rev. Lett.* **1990**, *65*, 1905-1908.